Prospects of Cuffless Pulse Pressure Estimation from a Chest-Worn Accelerometer Contact Microphone

Arash Shokouhmand[1], Haoran Wen[2], Samiha Khan[3], Joseph A. Puma[4], Amisha Patel[4], Philip Green[4], Farrokh Ayazi[2,5], Negar Ebadi[1]

[1]Stevens Institute of Technology, Hoboken, USA
[2]StethX Microsystems Inc., [5]Georgia Institute of Technology, Atlanta, USA
[3]New York Institute of Technology, [4]Sorin Medical P.C., New York, USA

Abstract

This study explores the correlation between pulse pressure (PP) and heart sounds on the chest wall. The proposed framework leverages a sensitive accelerometer contact microphone (ACM) to record chest vibrations. A discrete wavelet transform (DWT) decomposes the chest vibration recordings into a set of sub-bands, from which several time-domain features are extracted. An extreme gradient boosting (XGBoost) regressor is trained on the feature space for PP estimation, and the estimated values are compared with PP readings from a standard cuff-based blood pressure monitor. The performance of the model is evaluated on 20 patients with cardiovascular diseases (CVDs). Average root mean square error (RMSE), mean absolute error (MAE), and accuracy of 11.41 (± 6.42) mmHg, 10.49 (± 6.73) mmHg, and 77.14% (± 19.09%) are achieved, respectively, for a leave-subject-out validation. Additionally, the performance of the model is assessed through a 10-fold cross validation where an average accuracy of 95.68% is obtained, implying high consistency with ground-truth values. The most significant signal sub-bands for PP estimation are found to be high-frequency bands such as 1-2 kHz and 512-1,024 Hz, as well as medium-frequency bands of 32-64 Hz and 64-128 Hz. It is also demonstrated that the most contributive sub-band to PP estimation is 1-2 kHz.

1. Introduction

Cardiovascular diseases (CVDs) are the leading cause of mortality in the world, accounting for 32% of deaths in 2019 [1]. Early detection of CVD symptoms allows for timely risk management with proper interventions. Pulse pressure (PP), defined as the difference between the systolic and diastolic blood pressures, is among the most significant indicators of CVDs such as coronary heart disease [2].

Current blood pressure (BP) monitors employ an inflatable cuff to measure systolic and diastolic blood pressures. However, the intrusive nature of cuff-based BP monitors inhibits their use as a ubiquitous monitoring device. Recent advances in wearable sensors over the past decade have revolutionized blood pressure monitoring [3]. Several research works have addressed blood pressure estimation by introducing surrogates of pulse transit time (PTT) [4] or pulse arrival time (PAT) [5] using an electrocardiography (ECG) or seismo-cardiography (SCG) sensor in conjunction with a photoplethysmography (PPG) sensor attached to the earlobe, fingertip, or toe. The simultaneous use of two sensors however, causes inconvenience for the subject, hence provoking the need for less-intrusive devices. On the other hand, the precision accelerometer contact microphone introduced recently in [6] has shown promise in identifying cardiovascular abnormalities such as peripheral artery disease [7], ejection fraction [8], and valvular heart diseases [9], [10], using a single sensor setup for recording thoracic recordings.

As demonstrated in [11], pulse pressure is proportional to the stroke volume, which is defined as the blood volume pumped from the heart per cycle. In this paper, we assume that changes in the stroke volume appear as changes in the energy level of heartbeat-induced vibrations on the chest wall. Hence, measuring these changes could potentially enable the estimation of pulse pressure. In this work, for the first time we estimate pulse pressure using a single sensitive accelerometer contact microphone (ACM) placed on the chest wall.

This paper is organized as follows: Section 2 describes the experimental setup, data collection procedure, and signal processing chain designed for the estimation of pulse pressure from chest wall recordings. Section 3 discusses the experimental results. The paper is concluded in Section 4, where future directions are also discussed.

2. Experimental Setup and Methodology

2.1. Data Collection

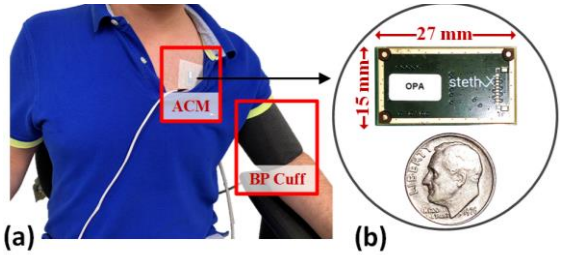

Fig. 1. (a) Experimental setup including an accelerometer contact microphone (ACM) attached to the pulmonary region and an expanded-coverage, preformed blood pressure cuff (OMRON HEM-FL31) secured around the left arm as reference. (b) The dimensions of the ACM sensor head.

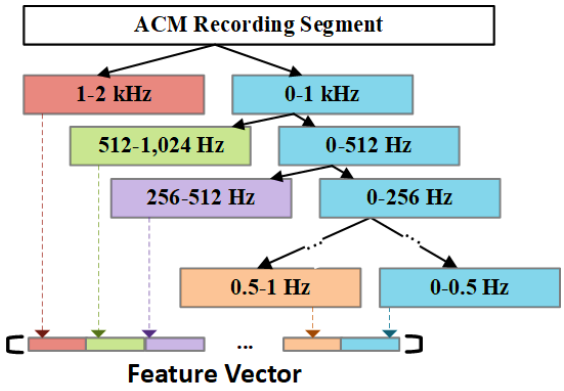

Fig. 2. Feature extraction using signal decomposition based on discrete wavelet transform (DWT). Wavelet sub-bands are used for feature extraction.

In this work, twenty subjects with cardiovascular diseases (CVDs), consisting of nine male and eleven females, are studied at the cardiac care unit of Sorin Medical P.C. in New York City. The average (± standard deviation) age, height, and weight of the patients are 70.25 (± 10.77) years, 167.04 (± 12.09) cm, and 82.32 (± 22.07) kg, respectively.

As shown in Fig. 1 (a), the experimental setup consists of a ± 4 g sensitive accelerometer contact microphone (ACM) with micro-g resolution and small form-factor of 27 mm × 15 mm × 2.5 mm (Fig. 1 (b)) from StethX Microsystems [12], which is attached to the pulmonary region of the subjects using medical-grade adhesive tape. This device is a low-noise accelerometer with a wide operational bandwidth of 0-10 kHz, allowing for recording heartbeat-induced sounds and vibrations on the chest wall. The device is not sensitive to airborne emission sounds, making it a robust phonocardiogram sensor against acoustic ambient noise. The subjects were seated at rest on a chair for a period of five minutes, followed by five minutes of ACM measurements at a sampling rate of 22.33 kHz, still at a seated position. Immediately afterwards, an OMRON-BP786N blood pressure monitor was used to measure the systolic blood pressure (SBP) and diastolic blood pressure (DBP) of the subjects from their left arms. Pulse pressure was then calculated by subtracting the DBP from SBP. The patient experimental protocol was approved by the Institutional Review Board of Stevens Institute of Technology under protocol number 2022-044 (N). The collected data were transferred to a computer and processed in a Python framework.

2.2. Signal Pre-processing

ACM recordings were initially band-pass filtered using a zero-phase, 3rd-order Butterworth filter over the frequency range of 2 Hz - 4 kHz to remove respiration artifacts and baseline wander. Filtered signals were then down-sampled to a sampling rate of 4 kHz to reduce the computational complexity of the processing steps. Subsequently, ACM signals were segmented into 10-second time frames similar to our previous work [13]. The data segmentation procedure was carried out twice, employing two different approaches. The first approach involved 90% overlap between consecutive segments, while the second approach utilized a 10-second gap between segments. The latter strategy was performed to prevent data leakage and ensure the integrity of the results. Finally, segments contaminated with motion artifacts due to movements during recordings were removed from ACM signals by applying a root-mean-square (RMS) filter with a sliding window of 500 ms for signal segmentation. The segment removal threshold was selected as twice the median value of the filter, setting the criterion for discarding the segments which exceeded the threshold level. The resulting motion-free signal segments were used for feature extraction.

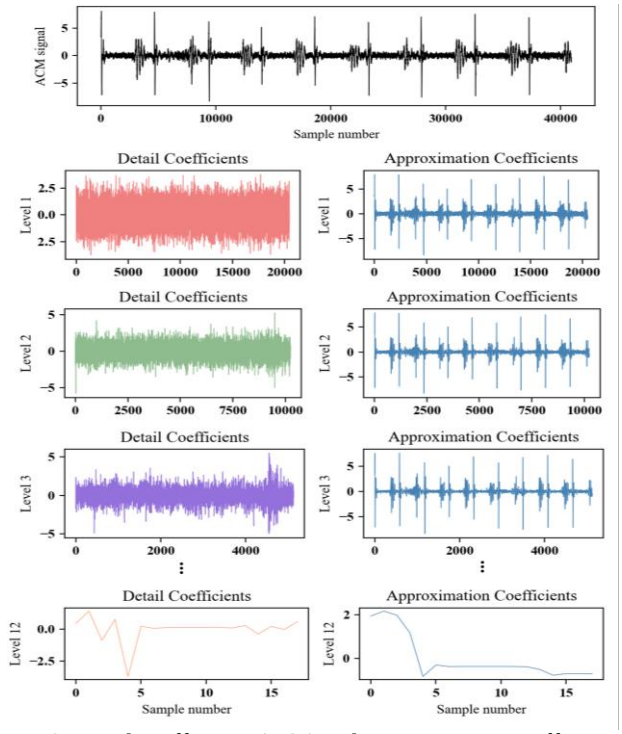

Fig. 3. Detail coefficienis (DCs) and approximation coefficients (ACs) of a 10-sceond ACM signal segment achieved by 12-level DWT decomposition.

2.3. Feature Extraction from ACM Recordings

As mentioned in Section 1, variations in heartbeat-induced vibrations on the chest wall contribute to pulse pressure estimation. The vibration on the chest wall can be directly recorded by the ACM, enabling the investigation of time-domain features. In order to characterize the ACM recordings, discrete wavelet transform (DWT) with a symlet kernel is employed to decompose the segments into 12 sub-bands (levels) for feature extraction, as illustrated in Fig. 2. At each decomposition level, the segments are split into high-frequency and low-frequency time series with coefficients

called detail coefficients (DCs) and approximation coefficients (ACs) respectively, as depicted in Fig. 3.

In this work, we extract features from 12 detail coefficient sets corresponding to 0.5-1 Hz, 1-2 Hz, 2-4 Hz, 4-8 Hz, 8-16 Hz, 16-32 Hz, 32-64 Hz, 64-128 Hz, 128-256 Hz, 256-512 Hz, 512-1024 Hz, and 1-2 kHz. Additionally, features from the coefficient set associated with 0-0.5 Hz are appended to the feature vector to provide a comprehensive representation of the segment within the whole frequency range. Per signal segment, features include the mean, standard deviation, skewness, kurtosis, 10th percentile, 25th percentile, 50th percentile, 75th percentile, and 90th percentile of the absolute and squared values of 13 coefficient sets (i.e., $13\times 2\times 9$ features). Furthermore, the differences between every pair of the afore-mentioned percentiles are incorporated in the feature space (i.e., $13\times 2\times 10$ features). As such, each 10-second signal segment is represented by a total of 494 features.

2.4. Regression Model for Pulse Pressure Estimation

According to our sample size, a machine learning regression model based on the extreme gradient boosting (XGBoost) method was implemented to estimate pulse pressure values from the extracted features. This model employs ensemble decision trees to minimize the regression error. XGBoost was trained on the sample space to minimize the square error loss function between the predicted and ground-truth pulse pressures. The model was optimized using the gradient descent method.

3. Experimental Results and Discussion

A total of 474 and 8,275 segments are obtained from 20 patients with an average (± standard deviation) pulse pressure of 49.15 (± 11.83) mmHg for non-overlapped and 90%-overlapped data, respectively. It has been demonstrated that pulse pressure is inversely proportional to the pulse arrival time (PAT) [11]. In this study, since the subjects are at rest, PAT is assumed to be constant over the short duration of measurement. As such, the segments corresponding to each subject are labeled by the same pulse pressure value calculated as the difference between the measured SBP and DBP. Two validation strategies are adopted to evaluate the performance of the predictive model. The first strategy is 20-fold leave-subject-out validation (LSOV), where the model is trained on the data of 19 subjects and tested on the remaining held-out subject. The second strategy is 10-fold cross-validation (10-CV), where the non-overlapped data is divided into two parts; 426 segments (90%) are used for training and the remaining 48 segments (10%) constitute the test set. The LSOV method differs from 10-CV in the sense that LSOV considers the dependence among the segments corresponding to the same subject, whereas 10-CV assumes that segments of the same subject are independent. Although 10-CV has been widely used in the literature, LSOV offers a more realistic evaluation. In the remainder of the paper, performance evaluation is reported for both validation strategies.

Table 1. Performance Evaluation of the Pulse Pressure Estimation Framework.

Metric	Blood Pulse Pressure Estimation Error (± Standard Deviation)	
	Leave-Subject-Out Validation	Cross-Validation (10-Fold)
RMSE (mmHg)	11.41 (± 6.42)	2.15 (± 0.71)
MAE (mmHg)	10.49 (± 6.73)	1.87 (± 0.38)
Acc. (%)	77.14 (± 19.09)	95.68 (± 1.17)

3.1. Pulse Pressure Estimation Evaluation

Table 1 summarizes the performance of the proposed pulse pressure estimation framework in terms of root mean square error (RMSE), mean absolute error (MAE), and accuracy (Acc.), defined as the percentage of relative error. Average RMSE values of 11.41 mmHg and 2.15 mmHg for LSOV and 10-CV, respectively, suggest robust estimation of pulse pressure. Similarly, MAE values of 10.49 mmHg and 1.87 mmHg respectively reported for LSOV and 10-CV demonstrate high linear consistency between the actual pulse pressure and associated predictions. This consistency is further confirmed by average accuracies of 77.14% and 95.68% achieved for LSOV and 10-CV, respectively. The relatively small difference between the performance achieved for LSOV and 10-CV suggests that the predictive model could take advantage of pre-knowledge about the subject's cardiac cycle and the corresponding pulse pressure values for the accurate estimation of pulse pressure. This is potentially obtained by fine-tuning the predictive model on a few seconds of the subject's recordings and the corresponding pulse pressure readings.

The authors in [14] have reported average RMSEs of

Table 2. Contributive Frequency Bands for Pulse Pressure Estimation.

Number	Sub-bands Contributions	
	Band Score	Frequency Sub-band
1	**156**	**1-2 kHz**
2	**37**	**512–1,024 Hz**
3	**19**	**64–128 Hz**
4	**17**	**128–256 Hz**
5	**14**	**32–64 Hz**
6	**11**	**16–32 Hz**
7	7	256–512 Hz
8	7	4–8 Hz
9	6	2–4 Hz
10	5	8–16 Hz
11	2	0.5–1 Hz
12	1	1–2 Hz
13	1	0–0.5 Hz
Average	**21.76**	**N/A**

3.59 mmHg and 2.24 mmHg for the static squat exercise and the cold pressor test, respectively, based on 5-fold cross-validation of 11 healthy subjects. Considering the 2.15 mmHg RMSE achieved on 20 CVD patients in this study, the proposed pulse pressure estimation framework shows promise for CVD patients with wide ranges of PP.

3.2. Significant Frequency Sub-Bands

The contribution of each frequency sub-band to pulse pressure estimation is reported in Table 2. For each subject in LSOV, the features are ranked based on their occurrence frequency in the ensemble trees. A feature is selected as highly contributive if its frequency exceeds the following threshold:

$$\tau = \sigma + \delta, \quad (1)$$

where σ and δ represent the average and standard deviation of the frequency distribution, respectively. The top features from all subjects are then combined, and the frequency of each feature is calculated again. Finally, a band score is calculated based on the occurrence of each frequency sub-band in the combined list as summarized in Table 2. According to this table, the most and least contributive frequency bands are 1-2 kHz and 0-0.5 Hz with scores of 156 and 1, respectively. It is also demonstrated that the medium frequency band 64-128 Hz with a band score of 19 suggests higher correlation with PP compared to high-frequency bands such as 256-512 Hz with a band score of 7.

4. Conclusion and Future Works

This paper explores the relation between pulse pressure and heart sounds acquired by a sensitive accelerometer contact microphone (ACM). It is demonstrated that blood pulse pressure can be predicted using the features derived from the detail coefficients of the discrete wavelet transform with accuracies of 77.14% and 95.68% for leave-subject-out and 10-fold cross-validations, respectively. Furthermore, it is proven that while extracted features from high-frequency bands such as 1-2 kHz and 512-1,204 Hz are the most consistent with pulse pressure values, medium frequency bands such as 64-128 Hz and 32-64 Hz are also contributive to the estimated values.

In our future studies, the performance of the system will be evaluated on a diverse range of individuals to investigate generalizability and robustness of the model. Having a large amount of data also allows for using state-of-the-art deep-learning techniques to directly relate the underlying patterns in ACM recordings to pulse pressure values. Another research direction involves investigating the potential applications of the system beyond pulse pressure estimation. ACM recordings could be used to predict other hemodynamic parameters such as the aortic valve area, which have important clinical implications.

References

[1] W. H. O. (WHO), "WHO reveals leading causes of death and disability worldwide: 2000-2019," *(WHO), World Health Organization*, 2020. https://www.who.int/news/item/09-12-2020-who-reveals-leading-causes-of-death-and-disability-worldwide-2000-2019.

[2] S. S. Franklin, S. A. Khan, N. D. Wong, M. G. Larson, and D. Levy, "Is pulse pressure useful in predicting risk for coronary heart disease? The Framingham Heart Study," *Circulation*, vol. 100, no. 4, pp. 354–360, 1999.

[3] T. Arakawa, "Recent research and developing trends of wearable sensors for detecting blood pressure," *Sensors*, vol. 18, no. 9, p. 2772, 2018.

[4] C.-S. Kim, A. M. Carek, R. Mukkamala, O. T. Inan, and J.-O. Hahn, "Ballistocardiogram as proximal timing reference for pulse transit time measurement: Potential for cuffless blood pressure monitoring," *IEEE Trans. Biomed. Eng.*, vol. 62, no. 11, pp. 2657–2664, 2015.

[5] W. Chen, T. Kobayashi, S. Ichikawa, Y. Takeuchi, and T. Togawa, "Continuous estimation of systolic blood pressure using the pulse arrival time and intermittent calibration," *Med. Biol. Eng. Comput.*, vol. 38, pp. 569–574, 2000.

[6] P. Gupta, M. J. Moghimi, Y. Jeong, D. Gupta, O. T. Inan, and F. Ayazi, "Precision wearable accelerometer contact microphones for longitudinal monitoring of mechano-acoustic cardiopulmonary signals," *NPJ Digit. Med.*, vol. 3, no. 1, pp. 1–8, 2020.

[7] A. Shokouhmand *et al.*, "Diagnosis of Peripheral Artery Disease Using Backflow Abnormalities in Proximal Recordings of Accelerometer Contact Microphone (ACM) (Cover Article)," *IEEE J. Biomed. Heal. Informatics*, vol. 27, no. 1, pp. 274–285, Jan. 2023, doi: 10.1109/JBHI.2022.3218595.

[8] A. Shokouhmand *et al.*, "Detection of Left Ventricular Ejection Fraction Abnormality Using Fusion of Acoustic and Biopotential Characteristics of Precordium," in *2022 IEEE Sensors*, 2022, pp. 1–4.

[9] A. Shokouhmand *et al.*, "Diagnosis of Coexisting Valvular Heart Diseases Using Image-to-Sequence Translation of Contact Microphone Recordings," *IEEE Trans. Biomed. Eng.*

[10] B. Sang *et al.*, "Detection of Normal and Paradoxical Splitting in Second Heart Sound (S2) using a Wearable Accelerometer Contact Microphone," in *2022 IEEE Sensors*, 2022, pp. 1–4.

[11] Z. Tang *et al.*, "A chair–based unobtrusive cuffless blood pressure monitoring system based on pulse arrival time," *IEEE J. Biomed. Heal. informatics*, vol. 21, no. 5, pp. 1194–1205, 2016.

[12] P. Gupta, H. Wen, L. Di Francesco, and F. Ayazi, "Detection of pathological mechano-acoustic signatures using precision accelerometer contact microphones in patients with pulmonary disorders," *Sci. Rep.*, vol. 11, no. 1, pp. 1–12, 2021.

[13] A. Shokouhmand, N. D. Aranoff, E. Driggin, P. Green, and N. Tavassolian, "Efficient Detection of Aortic Stenosis Using Morphological Characteristics of Cardiomechanical Signals and Heart Rate Variability Parameters," *Sci. Rep.*, vol. 11, no. 1, 2021.

[14] J. Lee, J. J. Sohn, J. Park, S. M. Yang, S. Lee, and H. C. Kim, "Novel blood pressure and pulse pressure estimation based on pulse transit time and stroke volume approximation," *Biomed. Eng. Online*, vol. 17, no. 1, pp. 1–20, 2018, doi: 10.1186/s12938-018-0510-8.

Address for correspondence:
Negar Ebadi (formerly Negar Tavassolian)
Department of Electrical and Computer Engineering, Stevens Institute of Technology, Hoboken, NJ 07030, USA.
negar.ebadi@stevens.edu